
Realizing Disentanglement in LM Latent Space via Vocabulary-Defined Semantics

Jian Gu¹, Aldeida Aleti¹, Chunyang Chen², and Hongyu Zhang³

¹Monash University, jian.gu, aldeida.aleti@monash.edu

²Technical University of Munich, chun-yang.chen@tum.de

³Chongqing University, hyzhang@cqu.edu.cn

Abstract

Understanding the latent space of language models (LMs) is important for improving the performance and interpretability of LMs. Existing analyses often fail to provide insights that take advantage of the semantic properties of language models and often overlook crucial aspects of language model adaptation. In response, we introduce a pioneering approach called vocabulary-defined semantics, which establishes a reference frame grounded in LM vocabulary within the LM latent space. We propose a novel technique to compute disentangled logits and gradients in latent space, not entangled ones on vocabulary. Further, we perform semantical clustering on data representations as a novel way of LM adaptation. Through extensive experiments across diverse text understanding datasets, our approach outperforms state-of-the-art methods of retrieval-augmented generation and parameter-efficient finetuning, showcasing its effectiveness and efficiency.

1 Introduction

Large-scale language models are drawing significant attention both due to their potential opportunities and associated risks [1]. Technically, the performance of LMs may be greatly affected by the entanglement issue in LM latent space [2, 3]. Latent space is a high-dimensional space where linguistic patterns, relations, and features are encoded, enabling the model to process and understand language. Considering its essential role in LMs, potential progress in this direction will contribute to the study of both data and models. Entanglement indicates the phenomenon where the elements of a vector data correlate to each other. In contrast, disentanglement means the case where the elements are independent of each other. For example, LM latent representations, namely distributed representations (such as [0.1, 0.3, 0.4, 0.2]), are entangled while onehot embeddings (such as [0, 0, 1, 0]) are disentangled. The inputs and outputs of LMs are disentangled data of a huge dimension (corresponding to the vocabulary size), while the latent representations of LMs are entangled data of a smaller but still very high dimension (corresponding to the dimension size of latent space). The entanglement in latent space derives the gap between machine-friendly features (e.g. embeddings, representations) and human-friendly results (e.g. tokens, pixels). The gap determines the performance of LMs and the human confidence in LMs. Consequently, the extent to which this gap is minimized influences not only the technical efficacy of LMs but also their reliability in various practical applications.

Centered on the entanglement issue in latent space, we introduce two related scenes: LM forward-pass and LM backward-pass, by respectively studying logits and gradients. And then, we will discuss the challenges of solving the issue, and give our countermeasures. In LM forward-pass, the (disentangled) logits is computed on LM vocabulary, then by checking the loss, we will know how far the prediction is to the ground truth. However, the concept of logits does not exist in the latent space. Or else, we will know on-the-fly how good the latent representations are, and further, optimize them in agile. The entangled representation in latent space is not logits and cannot take the role of logits, even though it

Preprint. Under review.

is in the logits computation. In LM backward-pass, the (disentangled) gradients is computed on LM vocabulary, and then backpropagates to model layers. However, limited by the dimension of latent space, which is smaller than the vocabulary size, and also the meaning of dimension is different, the gradients in latent space become entangled. It means, we always have to take the LM-head into consideration to exactly optimize the representations in latent space.

The first challenge is to obtain the logits in LM latent space. Previous work has primarily employed sampling and probing techniques [2, 4], such as predicting the semantic meaning of a given latent representation based on its neighboring representations. However, the semantics property of LMs is not adequately utilized. While such methods are sufficient for data analysis, they fall short in terms of optimizing the model itself. By examining the distribution of data representations in the latent space of LMs, we can identify potential outliers and the misprocessed data. However, it is hard to have clear insights into LMs, such as offering guidance on improving their performance.

The second challenge lies in disentangling the gradients in LM latent space. In the common practices of two important LM techniques: retrieval-augmented generation (RAG) and parameter-efficient fine-tuning (PEFT), they tend to either introduce new deviations from data or ignore the deviations of LM-head. For RAG, the practice is retrieving the most referenceable data to assist LMs, but this practice tends to introduce deviations of the data into LM inference, despite its potential to mitigate the deviations of LM-head. For PEFT, the adaptation is centered on fine-tuning the partial but essential parameters in the LM layers. However, due to its huge size and special role, the LM-head matrix tends to be excluded from fine-tuning. It increases the burden of fine-tuning, since more parameters are updated to compensate for the effect of directly fine-tuning the LM-head.

To resolve the above-mentioned issues, in this paper, we propose a novel, intuitive, and effective approach to formulate the semantics of LM latent space: *Vocabulary-Defined Semantics*, short as *VDS*. In particular, we propose the following countermeasures: (1) we define the semantic basis in the latent space, as a reference frame of LM semantics property, to realize the disentanglement; (2) we treat the labels (ground truth) in the LM vocabulary as the referenceable data, to avoid deviations of the retrievable data; (3) we propose a novel practice to compute the logits, aiming to transform the adaptation of the LM-head matrix into refining latent representations. In addition, we have conducted large-scale experiments and detailed analysis across diverse datasets of text understanding, with two families of LMs. Based on our results, our approach outperforms the SOTAs of PEFT and RAG in both effectiveness and efficiency. The replication repository is attached as supplementary material.

Our contributions are as follows:

- (in concept) we propose defining a group of special representations for disentangled semantics (termed as “semantic basis”). Compared to prior work of analyzing the semantics of data from an entangled perspective, the analysis with semantic basis is intuitive;
- (in theory) we propose a novel way to compute logits, via similarity measurement instead of common matrix multiplication. The practice is supported by the local isotropy of LM latent space. It can realize the disentanglement effects on gradients;
- (in practice) we propose using representation clustering to realize LM adaptation. We use a lightweight neural clustering module to refine the data representations semantically. It is equivalent to incorporating the LM-head matrix into fine-tuning.

2 Related Work

Generally, retrieval-augmented methods combine data retrieval and LM for better performance, such as in-context learning, which prompts LM with the retrieved task demonstrations. The demonstrations are in the form of an input-output pair, and will compose with the given input as the new input. The retrieval is conducted based on the similarity of the corpus data to the given input. Similarly, the data to retrieve can be the context with the potentially related background. The general practice of similarity measurement in data retrieval is based on embeddings or representations, but KP evaluates the similarities of data based on the logits. Besides, KP retrieval the same amount of data for each label in the vocabulary for balance. Similar to retrieval-augmented methods, nearest-neighbor methods use the retrieval technique for improvements as well. However, it happens at the output side, such as the LM last-layer, instead of the input side. The data to retrieve is key-value pairs, for

example, let the representation be the key and the corresponding ground truth be the value. The given representation is used as the query to retrieve the related history data. Then LM does inference with hybrid logits: one is from the model prediction while the other one is from the nearest-neighbor retrieval. The hybrid logits will be used to compute a normalized probability distribution. It has been used for language modeling in k NN-LM [5] and machine translation in k NN-MT [6]. A similar practice is using activations as the key [7]. A further topic along this direction is to realize retrieval-based neuro-symbolic inference, such as RETOMATON [8].

To reduce the computation cost of finetuning large-scale LMs, and the storage cost of the finetuned models, PEFT methods are proposed. They only update partial parameters. Besides, compared with fully finetuning, PEFT methods can better avoid catastrophic forgetting [9], and learn better from a small amount of data. Adapter methods directly introduce new modules to the LMs, such as bottleneck adapters [10] and compacter [11]. PROMPT TUNING prepends tunable tokens to the input data. Similarly, PREFIX-TUNING modifies the multi-head attention with new parameters, that is, prepending trainable vectors to the key and value matrices. LORA [12] uses low-rank matrix to learn the additive updates on the self-attention weight matrix, while its variants are improving the parameter efficiency, such as ADALORA [13], DORA [14]. While IA³ [15] rescales the activations by tuning additional coefficients. In addition, some work is the combinations of other PEFT methods [16]. For example, mix-and-match adapters are a combination of prefix-tuning and bottleneck adapters [17].

3 Semantics of LM Latent Space

The motivation of our approach is to realize the disentanglement of gradients. On the definition of disentanglement (of a representation or vector-form data) [18], intuitively speaking, if the meaning to be conveyed by a single element is independent of the other elements, then the data is disentangled (e.g. onehot representation), otherwise it is entangled (e.g. distributed representation). There are two reasons to disentangle gradients: (1) In LM adaptation, LM-head matrix is often avoided being finetuned since it has a large number of parameters (which is the product of dimension size and vocabulary size). However, the module in charge of LM outputs, so it deserves to be finetuned for better performance; (2) The gradients will be entangled when passing through the LM-head matrix in backpropagation, so it is hard to optimize the loss of a specified representation with the corresponding ground truth solely. Each time of loss computation will require the logits computation on the whole vocabulary, which indicates a huge waste in the costs.

In general practice, the logits and gradients are obtained *after* the LM-head, In the LM forward-pass, the logits is obtained by the multiplication between the last-layer latent representation and the LM-head matrix, and then is compared with the ground truth to compute the loss. Further, in the backward-pass, the loss will propagate the gradients back from the LM-head to the embeddings layer. The gradients is disentangled initially and each element represents the value difference between the corresponding element in the logits with the ground truth. When passing through the LM-head matrix, its dimension size is reduced. The reduction in dimension size indicates the meaning of each element is no longer independent of each other, which indicates an entanglement.

As a solution, we propose computing logits and gradients in the LM latent space, not on the vocabulary. That is, excluding the LM-head matrix from the logits computation. In our approach, the logits and gradients are obtained *before* the LM-head. First, we obtain the corresponding representations of vocabulary labels by solving the pseudoinverse matrix of LM-head, and treat such representation as “semantic basis”. Then, leveraging the local isotropy of LM latent space, we compute logits via similarity measurement, namely the similarities between latent representations and semantic bases. Therefore, we can compute logits and further compute the gradients in the latent space. In backpropagation, LM-head is executed, so the dimension size of the disentangled gradients will not change. To examine the effects of gradients disentanglement, namely the mentioned effectiveness and efficiency, we define LM adaptation as representation clustering, where the cluster centroids are specified as the semantic bases beforehand. Leveraging a high-dimensional transformation, we will refine the last-layer latent representations to let them be closer to the ground truth.

Let’s demonstrate with an LM, whose vocabulary consists of five colorful labels, as shown in Figure 1: (1) On the semantic basis (see the upper-left), we obtained the semantic bases in the latent space, represented by large color dots. The colors correspond to the labels in the vocabulary one to one; (2) On the semantic logits (see the upper-right), we use a small dark dot to represent a representation from

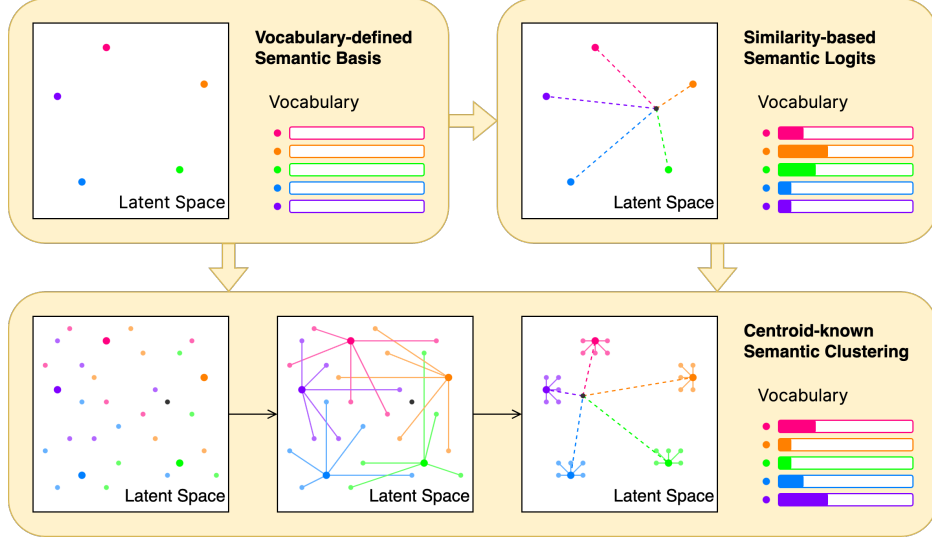


Figure 1: The Illustration of Semantic Basis, Semantic Logits, and Semantic Clustering.

the test set. We measure its similarities with the semantic bases as logits. The logits are normalized as distribution in the vocabulary, and the argmax label is *orange*; (3) On the semantic clustering (see the bottom), we use small color dots to represent the representations from the training set, and their colors indicate the corresponding ground truth. Originally, the small dots were mixed and scattered all around. We learn a transformation to gather them by color, into clusters centered in the corresponding semantic basis. The clustering is on the whole latent space, affecting the representations from the test set, so the dark dot also moved. The logits of the dark has changed, and its argmax label is now *violet*.

3.1 Vocabulary-defined Semantic Basis

In LM latent space, the semantics of data representations is computed via similarity measurement. In the common way of logits computation, the data representation is projected to the LM vocabulary, and its actual semantic meaning is represented by the probability distribution on the vocabulary. Given this, we propose to use the vocabulary to model the semantics of LM latent space.

First, we define heuristic logits of disentangled semantic meanings. We take onehot embeddings as the most semantically representative distributions of the vocabulary. Assuming a vocabulary of size v , we need v unique semantic bases to represent v different semantic meanings. Since the softmax operation maintains monotonicity, we can further regard the onehot distributions as onehot logits.

Then, we compute the corresponding representation of the onehot logits. For a given LM-head matrix, we conduct matrix multiplication to get the corresponding representation in the latent space. Since we compute the representations with the logits and the LM-head, instead of using the LM-head matrix \mathbb{W} , we use its pseudoinverse \mathbb{W}^+ . At the output side of LM, we multiply the onehot logits \vec{l} by the pseudoinverse matrix \mathbb{W}^+ to obtain the corresponding representation \vec{r} . Expressed in formula, that is, $\vec{r} = \vec{l} \cdot \mathbb{W}^+$. The computation is equivalent to solving the least squares problem of a system of linear equations. We call each of the obtained vectors *semantic basis*.

3.2 Similarity-based Semantic Logits

The latent space of Transformer models is proved to be locally isotropic [19], in terms of information and semantics. Therefore, we can convert the logits computation of LMs from matrix multiplication to distance measurement. Isotropy means that the properties of a space are uniform in all directions. That is, in different directions of the latent space, the semantic differences of representations in the same distance remain close. Therefore, when we consider all semantic bases, instead of only one basis, the hypothesis is almost true that *the similarity of representations in the latent space remains positively correlated with the similarity of the corresponding distributions on the vocabulary*.

Algorithm 1 Similarity-based Semantic Logits

Require: n semantic bases \vec{b}_i ; representation \vec{r}
Ensure: probability distribution $probs$ on the vocabulary
 $logits \leftarrow \text{init_1d_tensor}(n)$
for $i \leftarrow 0$ **to** $n - 1$ **do**
 $logits[i] \leftarrow \text{similarity_metric}(\vec{b}_i, \vec{r})$
end for
 $probs \leftarrow \text{softmax}(logits)$

Similarity-based Semantic Logits. For a given representation, the logits is commonly computed by multiplying with the LM-head matrix, a novel practice is to compute its projection to the semantic bases using cosine similarity. Leveraging the positive correlation between the representation similarity in the latent space and the distribution similarity on the vocabulary, we compute the logits based on their similarities with the semantic bases. The similarity metric tends to be the cosine similarity, so the logits indicate the projections to the semantic bases. Further, the logits can be used to compute the probability distribution in the vocabulary, as shown in Algorithm 1.

3.3 Centroid-known Semantic Clustering

For an LM latent space scattered with data representations, the general LM adaptation process can be realized by *clustering* them centered on the corresponding semantic bases. In our approach, we specify each semantic basis as the oracle centroid of each cluster. In the optimal situation of LM adaptation, the last-layer representations of the same semantic meaning (corresponding to the same label), should stay in the same cluster. We call the process *semantic clustering*, short as SC. It can be taken by non-neural methods. We adopt a learning-based neural clustering method, because we can study more on similarity-based logits (as discussed in Section 5).

$$\lambda(\vec{r}) = \text{LN}(\text{MLP}(\text{CA}(\vec{r}))) \tag{1}$$

$$\text{CA}(\vec{r}) = \vec{r} \odot (\text{Bn}(\text{avg}(\vec{r})) + \text{Bn}(\text{max}(\vec{r}))) \tag{2}$$

In our approach, we introduce a simple neural clustering module into the LM for semantic clustering. The clustering module consists of a multi-layer perceptron (MLP), a channel attention (CA), and a layer normalization (LN), as shown in Equation (1). The channel attention learns the coefficients of the representations, based on the information in the channel domain [20], as shown in Equation (2). The coefficients are a sum of the Bottleneck (Bn) outputs, respectively on the average-pooling (avg) and the maximum-pooling (max) of the representations. While the perceptron and normalization learn a non-linear transformation in the latent space.

4 Experiments

We conduct the experiments on diverse datasets and a wide range of GPT2 and Pythia scales. The details of language models and datasets are in Appendix A.

4.1 Setup

Models. We use recognized open-source LMs and involve two LM families in our experiments, one is the GPT2 series (117M-1.5B) [21], and the other one is the Pythia [22] series (160M-7B).

Datasets. We perform evaluation with established text understanding tasks, respectively for text classification: AGNews [23], SUBJ [24], TREC [25], and WebSS [26]; sentiment analysis: MR [27] and SST5 [28]; as well as similarity detection: MRPC [29].

Baselines. In our experiments, we study the effects of semantic clustering on general in-context learning, short as ICL [30]. Besides, we compare with the SOTA retrieval-augmented method, *KNN* prompting, short as KP [31]. We reproduce the practice of ICL and KP following the paper [31]. As an extension of the study, we also compare with parameter-efficient finetuning methods, including LORA [12] and IA³ [15], since we are involving a neural module to cluster representations.

TABLE 1: Accuracy on Text Understanding with RAG Methods.

Dataset	Method	GPT2				Pythia					
		Small	Medium	Large	XL	Small	Medium	Large	XL	3B	7B
AGNews	ICL	0.283	0.545	0.684	0.709	0.517	0.633	0.612	0.641	0.750	0.708
	KP	0.860	0.852	0.854	0.884	0.250	0.855	0.877	0.876	0.881	0.881
	SC	0.922	0.926	0.924	0.930	0.881	0.921	0.932	0.934	0.933	0.934
MR	ICL	0.558	0.534	0.793	0.567	0.548	0.806	0.537	0.844	0.851	0.891
	KP	0.706	0.742	0.847	0.803	0.500	0.815	0.857	0.859	0.865	0.885
	SC	0.781	0.843	0.863	0.876	0.500	0.772	0.849	0.874	0.879	0.870
MRPC	ICL	0.665	0.665	0.665	0.665	0.665	0.665	0.665	0.665	0.665	0.665
	KP	0.559	0.587	0.597	0.588	0.335	0.541	0.583	0.565	0.574	0.605
	SC	0.681	0.659	0.674	0.681	0.665	0.678	0.697	0.682	0.703	0.717
SST5	ICL	0.309	0.157	0.286	0.193	0.239	0.347	0.340	0.349	0.483	0.522
	KP	0.305	0.357	0.375	0.381	0.286	0.375	0.395	0.435	0.423	0.430
	SC	0.418	0.456	0.479	0.480	0.452	0.419	0.463	0.478	0.480	0.495
SUBJ	ICL	0.500	0.533	0.617	0.527	0.524	0.689	0.662	0.602	0.906	0.500
	KP	0.842	0.878	0.895	0.901	0.500	0.856	0.883	0.894	0.919	0.907
	SC	0.899	0.934	0.911	0.914	0.500	0.903	0.922	0.941	0.942	0.956
TREC	ICL	0.552	0.546	0.622	0.586	0.360	0.654	0.732	0.564	0.722	0.822
	KP	0.810	0.818	0.882	0.854	0.226	0.836	0.880	0.888	0.844	0.866
	SC	0.908	0.934	0.932	0.952	0.784	0.916	0.956	0.964	0.950	0.946
WebSS	ICL	0.315	0.313	0.208	0.266	0.181	0.432	0.492	0.514	0.496	0.522
	KP	0.740	0.776	0.763	0.791	0.132	0.776	0.801	0.807	0.805	0.843
	SC	0.792	0.796	0.818	0.811	0.132	0.807	0.845	0.807	0.829	0.807
Avg.	ICL	0.454	0.470	0.553	0.502	0.433	0.604	0.577	0.597	0.696	0.662
	KP	0.689	0.716	0.745	0.743	0.318	0.722	0.754	0.761	0.759	0.774
	SC	0.771	0.792	0.800	0.806	0.559	0.774	0.809	0.811	0.816	0.818

Metrics. We take *Accuracy* to evaluate the predictions. The value range is $[0, 1]$, the larger, the better.

4.2 Pipelines

In the experiments, we use few-shot prompts for RAG baselines, making full use of the LM context length. While for PEFT baselines and semantic clustering, we use zero-shot prompts to reduce the effects of in-context prompting. The prompt templates used in our experiments are available in Appendix A. On ICL, we retrieve the demonstrations randomly from the training set, and take the same number of demos for each class, making the full usage of the allowed context length. On KP, the practice is roughly the same, but the retrieval process is led by the KL divergence. The data similar in the probability distribution are more likely to be retrieved. On PEFT methods, we specify the recommended modules be trainable based on their papers (that is, QKV matrices in LORA, and QKV matrices plus the second FC layer in IA³), using the default hyperparameters (see Appendix A). On our approach SC, we freeze all LM parameters to merely train the neural clustering module.

4.3 Effectiveness Study

Compared to SOTA methods, semantic clustering is competitive. It outperforms others in almost all models and most datasets. SC performs not that well in Pythia-S. Compared with PEFT methods, SC merely performs slightly worse than IA³ in MRPC and SST datasets.

Based on the results shown in Table 1, on GPT2 models, SC obtained the optimal average performance, and KP takes the suboptimal position. Besides, SC outperforms the baseline ICL significantly. Compared with ICL, the improvements of SC are the least on MRPC, and are most obvious on AGNews and WebSS. Considering the number of classes is 2 in MRPC but 4 and 8 in AGNews and WebSS, SC have more effects when the number of classes is larger. On Pythia models, the findings are similar: SC obtained the optimal average performance on all datasets. In a few cases where the model is large enough (such as Pythia-7B), in MR and SST5 datasets, ICL perform slightly better; and in WEBSS, KP performs slightly better. However, their advantages is not common. On average, KP shows the suboptimal performance, better than ICL.

Based on the results shown in Table 2, our findings are similar. On most datasets, SC shows the best performance. And in Pythia-S, PYTHIA performs not that good. We have new findings on PEFT methods and LMs. In MRPC, SST5, and TREC, PEFT methods may perform as well as, or even better than SC. Based on our analysis, it is caused by the class balance of the data, as shown in Table 6. PEFT methods tend to perform better when the data amounts of different classes are different. In contrast, the performance of SC will not be affected by class balance. Besides, IA³ performs

TABLE 2: Accuracy on Text Understanding with PEFT Methods.

Dataset	Method	GPT2				Pythia					
		Small	Medium	Large	XL	Small	Medium	Large	XL	3B	7B
AGNews	LoRA	0.877	0.255	0.249	0.246	0.250	0.252	0.250	0.250	0.250	0.250
	IA ³	0.914	0.920	0.924	0.926	0.901	0.898	0.912	0.913	0.906	0.921
	SC	0.922	0.926	0.924	0.930	0.881	0.921	0.932	0.934	0.933	0.934
MR	LoRA	0.500	0.500	0.500	0.500	0.500	0.500	0.500	0.500	0.500	0.500
	IA ³	0.500	0.500	0.500	0.500	0.500	0.500	0.500	0.500	0.500	0.500
	SC	0.781	0.843	0.863	0.876	0.500	0.772	0.849	0.874	0.879	0.870
MRPC	LoRA	0.679	0.665	0.665	0.665	0.665	0.665	0.665	0.665	0.665	0.665
	IA ³	0.707	0.711	0.737	0.750	0.688	0.763	0.750	0.791	0.805	0.845
	SC	0.681	0.659	0.674	0.681	0.665	0.678	0.697	0.682	0.703	0.717
SST5	LoRA	0.478	0.387	0.176	0.231	0.257	0.221	0.238	0.226	0.176	0.200
	IA ³	0.517	0.538	0.567	0.582	0.489	0.531	0.568	0.583	0.583	0.608
	SC	0.418	0.456	0.479	0.480	0.452	0.419	0.463	0.478	0.480	0.495
SUBJ	LoRA	0.500	0.500	0.500	0.500	0.500	0.500	0.500	0.500	0.500	0.500
	IA ³	0.500	0.500	0.500	0.500	0.500	0.500	0.500	0.500	0.500	0.500
	SC	0.899	0.934	0.911	0.914	0.500	0.903	0.922	0.941	0.942	0.956
TREC	LoRA	0.946	0.958	0.382	0.188	0.646	0.646	0.328	0.454	0.368	0.426
	IA ³	0.930	0.952	0.968	0.966	0.902	0.960	0.954	0.964	0.966	0.962
	SC	0.908	0.934	0.932	0.952	0.784	0.916	0.956	0.964	0.950	0.946
WebSS	LoRA	0.132	0.132	0.132	0.132	0.132	0.132	0.132	0.132	0.132	0.132
	IA ³	0.137	0.173	0.132	0.136	0.178	0.132	0.132	0.132	0.132	0.178
	SC	0.792	0.796	0.818	0.811	0.132	0.807	0.845	0.807	0.829	0.807
Avg.	LoRA	0.587	0.485	0.372	0.352	0.421	0.417	0.373	0.389	0.370	0.382
	IA ³	0.601	0.613	0.618	0.623	0.594	0.612	0.617	0.626	0.627	0.645
	SC	0.771	0.792	0.800	0.806	0.559	0.774	0.809	0.811	0.816	0.818

better than LORA, because IA³ learns coefficients to rescale the activations while LORA only learns the difference of the self-attention weight matrix, so the former is not limited in the self-attention module. Checking the cases of GPT2 models and Pythia models, when the model size is similar, the performances of most methods remain close. Since the quality of representations is decided by the model capability, and model capability is revealed by the model size, the performance of Pythia-S might be caused by the low-quality representations. Given the hyperparameters of GPT2-S and Pythia-S are almost the same, including the number of layers, dimension size, and vocabulary size, as shown in Table 5, the representations of Pythia-S are harder than GPT2-S to cluster well, which may be caused by the size of training corpus if both models are fully trained.

Comparing the results in the two tables, it is noticeable to see both SC and KP outperform PEFT methods on average. The reason is that, when adapting LMs to the downstream data, the common finetuning practices tend to ignore the effects of the LM-head matrix. Different from the trainable LM layers, the LM-head matrix represents a perspective of the whole LM latent space. If the matrix stays unchanged, the LM adaptation in semantics will be limited. KP picks the demonstrations as referenceable data based on the logits, so can partially have the effects of finetuning the LM-head matrix, but also introduce unexpected deviations (from the referenceable data). In contrast, SC is a disentanglement process, since it uses the reference frame to compensate the perspective of LM-head. By optimizing the data representations, SC realizes finetuning the LM-head matrix equivalently.

4.4 Efficiency Study

Compared to SOTA methods, semantic clustering shows efficiency in both computation and storage costs. The neural clustering module is lightweight and the time cost is small. In logits computation, the computation cost of similarity-measurement logits is at the same level as matrix-multiplication logits. However, due to logits disentanglement of the former, we can reduce the size of LM vocabulary to a domain-specific one to save computations. Assume the size of LM vocabulary is v , and the number of actually-used LM labels is \bar{v} , compared with matrix-multiplication logits, the time cost of similarity-measurement logits can be reduced to \bar{v}/v . Further, the time cost can be reduced to $1/v$ by merely optimizing the similarity with the ground truth, while maintaining the performance.

On the computation cost, PEFT methods require the most, then KP, while SC requires the least. As shown in Table 3, based on the average time cost at the Avg. column, ICL is the fastest and only costs around 0.9 hours. Then, SC and KP take 1.1 and 2.8 hours respectively, while LORA and IA³ cost around 8 hours. The INFERENCE operation costs longer time in RAG methods, since ICL and KP are using few-shot prompts, and the prompts occupy the 1k-context (GPT2 LMs) and 2k-context (Pythia LMs). In contrast, PEFT methods and SC take zero-shot prompts so their inference is faster.

TABLE 3: Runtime on Text Understanding with Pythia-7B (in Hours).

Method	Operation	Dataset							Avg.
		AGNews	MR	MRPC	SST5	SUBJ	TREC	WebSS	
ICL	Inference	1.302	0.805	0.721	0.978	0.863	0.434	0.882	0.855
KP	Indexing	1.792	0.893	0.901	2.518	0.990	2.984	2.628	1.815
	Inference	2.163	0.943	0.829	0.959	0.999	0.259	0.944	1.014
LoRA	Training	20.813	6.160	4.031	6.000	5.833	3.895	6.632	7.623
	Inference	0.313	0.379	0.571	0.462	0.459	0.156	0.260	0.371
IA ³	Training	20.171	6.177	4.041	6.016	5.851	3.908	6.652	7.545
	Inference	0.315	0.383	0.575	0.466	0.463	0.158	0.263	0.375
SC	Clustering	2.698	0.850	0.437	0.843	0.798	0.577	0.959	1.023
	Inference	0.102	0.134	0.163	0.146	0.141	0.046	0.096	0.118

Besides, KP takes a retrieval operation on the indexed demonstrations so it is slower than ICL. As discussed, different from the computing logits via matrix-multiplication, SC computes logits via similarity-measurement, so the time cost of inference can be reduced to \bar{v}/v and even $1/v$. Except from ICL, besides INFERENCE, all methods have an additional operation. The indexing operation of KP finds high-quality demonstrations for few-shot prompting by analyzing the logits and the ground truth of training data. It consists of an LM forward-pass with few-shot prompts and the ranking of neighboring logits (measured by KL divergence). LORA and IA³ require LM forward-pass and LM backward-pass with zero-shot prompts, even though the amount of trainable parameters is small but the computation cost of backpropagation is still the same as full finetuning. In contrast, SC requires LM forward-pass but the backward-pass with zero-shot prompts is only on the neural clustering module. Besides, due to the disentanglement, the time cost of logits computation is also reduced.

On the storage cost, KP requires the most storage cost while PEFT methods and SC have much lower costs. For a given LM, assume its dimension size of latent representations is d , the number of LM layers is l , and the size of LM vocabulary is v . ICL has no additional storage. KP needs to store the logits of neighboring prompts from the corpus (namely the training set), for each label in the vocabulary, that is, $k * v * v$ when the number of nearest neighbors is k . As PEFT methods, LORA and IA³ store the additional trainable parameters. Taking their recommended setups, the amount of their parameters are $4 * r * d * l$ and $7 * d * l$, when the low-rank parameter is r . For our approach SC, the storage cost is the neural clustering module, that is, $\frac{33}{8} * d * d$. The number of trainable parameters consists of $4 * d * d$ for the MLP and $\frac{1}{8} * d * d$ for the Bn. It can be further reduced to $\frac{33}{8} * d$ via parameterized hypercomplex multiplication [32].

5 Analysis and Explanation

In the following, we take an ablation study to further discuss our semantic-based approach (especially similarity-based logits computation), centered on the aspects of LM inference, LM training, and disentanglement. We run experiments on the same datasets, with the Pythia-7B model. We use labels in the form of SC[LOSS][GEN] to distinguish different settings, where LOSS indicates the practice of logits computation in LM training, and GEN indicates the practice in LM inference.

Logits in LM Inference. In our approach SC, we compute logits via similarity measurement (short as sm) in LM inference and LM training, marked as SC[sm][sm]. By comparing with the common way of using matrix multiplication (short as mm) for logits computation in LM inference, we can see how similarity-based logits differ in LM forward-pass. Therefore, we prepare such a variant SC[sm][mm].

Logits in LM Training. By comparing with the common logits computation in LM training, we can see how similarity-based logits differ in LM backward-pass. Therefore, we prepare such a variant SC[mm][sm]. In addition, to validate the efficiency in computing similarity-based logits, we prepare another variant SC[gt-sm][sm], which merely measures the similarity between the latent representation and the semantic basis of the ground truth (short as gt), instead of all semantic bases.

Gradients Disentanglement. By amplifying and suppressing the logits values before loss computation, we can show the difference between entangled gradients and disentangled gradients, and further, reveal the effects of gradients disentanglement. We take a simple strategy to manipulate the logits, that is, applying the natural exponential function (short as exp) to the logits, and then, normalizing the results. In the implementation, it is equivalent to applying an additional *softmax* operation, which amplifies

TABLE 4: Accuracy of Ablation Study with Pythia-7B Model.

Aspect	Ablation	Dataset							Avg.
		AGNews	MR	MRPC	SST5	SUBJ	TREC	WebSS	
	SC[sm][sm]	0.934	0.870	0.717	0.495	0.956	0.946	0.807	0.818
LM Inference	SC[sm][mm]	0.933	0.870	0.717	0.492	0.956	0.948	0.804	0.817
LM Training	SC[mm][sm]	0.934	0.824	0.726	0.457	0.500	0.948	0.801	0.741
	SC[gt-sm][sm]	0.936	0.860	0.733	0.468	0.941	0.952	0.812	0.815
Disentanglement	SC[exp-mm][sm]	0.250	0.500	0.665	0.231	0.500	0.226	0.132	0.358
	SC[exp-sm][sm]	0.936	0.867	0.719	0.472	0.957	0.952	0.806	0.815

the largest values and suppresses small values. Therefore, we prepare such variants $SC[exp-mm][sm]$ and $SC[exp-sm][sm]$, for matrix multiplication and similarity measurement respectively.

Based on the results shown in Table 4, compared to our approach SC, $SC[sm][mm]$ has a similar performance while $SC[mm][sm]$ shows an obvious performance drop. The minor difference in the performance of SC and $SC[sm][mm]$ indicates the roughly equivalent effects of two ways of logits computation in LM forward-pass. It proves the correctness of our hypothesis on the correlations of the representations similarity and distribution similarity. In contrast, the performance difference between SC and $SC[mm][sm]$ indicates that similarity measurement is better than matrix multiplication in logits computation, when clustering the representations in LM latent space. Since the clustering is after all model layers but before the LM-head matrix, the performance drop in LM backward-pass is caused by the gradients backpropagation of the LM-head matrix. In LM finetuning, due to its huge parameter amount, LM-head tends to be frozen and excluded from finetuning. It shows that similarity-based logits guarantee the correctness of gradients backpropagation when LM-head is frozen.

In addition, the performance of $SC[gt-sm][mm]$ is close to that of SC. However, their computation costs are very different. Taking Pythia-7B as an example, there are 50432 labels in the vocabulary (even though it may be reduced to a smaller domain-specific one to save computation) and the dimension size is 4096, so each time doing logits computation, we need to measure the similarity between the latent space representation and each semantic basis. The computation cost is at the same level as doing the matrix multiplication but more costly, since the similarity measurement is not merely one vector multiplication. In contrast, $SC[gt-sm][mm]$ only measures the similarity once for each logits computation. It shows a huge computation advantage of similarity-measurement logits.

On the gradients disentanglement, compared with $SC[mm][sm]$, the performance of $SC[exp-mm][sm]$ shows a huge performance drop. In contrast, compared with SC, the performance of $SC[exp-sm][sm]$ is almost the same. The reason explaining the contrasting phenomena is the gradients disentanglement. For matrix-multiplication logits, the gradients is entangled so the it is sensitive to the value differences on vocabulary labels. As shown in $SC[mm][sm]$, the value difference caused by the frozen LM-head will affect the performance, so a larger value difference by the softmax operation will damage the performance as well. In contrast, for similarity-measurement logits, the gradients is disentangled so it shows better in robustness, and insensitive to the value differences on vocabulary labels. In addition, the performances of $SC[exp-sm][sm]$ and $SC[gt-sm][sm]$ are very close. It proves that similarity-measurement logits tends to keep stable even though the practice of logits computation may differ. It also indicates that similarity-measurement logits is mainly focusing the similarity between the representation and the semantic basis of the corresponding ground truth.

6 Conclusion

In this paper, we have proposed the concept of semantic basis. It indicates defining a reference frame to analyze the semantic property of LM latent space. We also propose the similarity-based logits to realize the gradients disentanglement. Further, we have proposed semantic clustering as a manner of LM adaptation. Based on our results, semantic clustering shows competitive in finetuning LMs, while being significant in the computation cost. Moreover, through our ablation study, similarity-based logic is numerically as good as the common way of logic computation, but better in robustness.

Our work obtains the disentangled logits and gradients in LM latent space. It is useful for model training, such as LM finetuning. Besides, it could benefit other tasks where the ground truth is used to supervise the latent representation, such as model verification. Based on our results, semantic clustering shows effectiveness and efficiency in LM adaptation. It outperforms prior work in RAG and PEFT. Meanwhile, semantic clustering is meaningful to nearest-neighbor methods, which may

further benefit neuro-symbolic methods. In the future, we will explore more topics where the LM semantic property can help, contributing to not only LM performance, but also LM interpretability.

Acknowledgements

We sincerely thank DUG Technology for providing the computing resources. Their support greatly facilitated our research efforts.

References

- [1] Rishi Bommasani, Drew A. Hudson, Ehsan Adeli, Russ Altman, Simran Arora, Sydney von Arx, Michael S. Bernstein, Jeannette Bohg, Antoine Bosselut, Emma Brunskill, Erik Brynjolfsson, S. Buch, Dallas Card, Rodrigo Castellon, Niladri S. Chatterji, Annie S. Chen, Kathleen A. Creel, Jared Davis, Dora Demszky, Chris Donahue, Moussa Doumbouya, Esin Durmus, Stefano Ermon, John Etchemendy, Kawin Ethayarajh, Li Fei-Fei, Chelsea Finn, Trevor Gale, Lauren Gillespie, Karan Goel, Noah D. Goodman, Shelby Grossman, Neel Guha, Tatsunori Hashimoto, Peter Henderson, John Hewitt, Daniel E. Ho, Jenny Hong, Kyle Hsu, Jing Huang, Thomas F. Icard, Saahil Jain, Dan Jurafsky, Pratyusha Kalluri, Siddharth Karamcheti, Geoff Keeling, Fereshthe Khani, O. Khattab, Pang Wei Koh, Mark S. Krass, Ranjay Krishna, Rohith Kuditipudi, Ananya Kumar, Faisal Ladhak, Mina Lee, Tony Lee, Jure Leskovec, Isabelle Levent, Xiang Lisa Li, Xuechen Li, Tengyu Ma, Ali Malik, Christopher D. Manning, Suvir Mirchandani, Eric Mitchell, Zanele Munyikwa, Suraj Nair, Avaniika Narayan, Deepak Narayanan, Benjamin Newman, Allen Nie, Juan Carlos Niebles, Hamed Nilforoshan, J. F. Nyarko, Giray Ogut, Laurel J. Orr, Isabel Papadimitriou, Joon Sung Park, Chris Piech, Eva Portelance, Christopher Potts, Aditi Raghunathan, Robert Reich, Hongyu Ren, Frieda Rong, Yusuf H. Roohani, Camilo Ruiz, Jack Ryan, Christopher R’e, Dorsa Sadigh, Shiori Sagawa, Keshav Santhanam, Andy Shih, Krishna Parasuram Srinivasan, Alex Tamkin, Rohan Taori, Armin W. Thomas, Florian Tramèr, Rose E. Wang, William Wang, Bohan Wu, Jiajun Wu, Yuhuai Wu, Sang Michael Xie, Michihiro Yasunaga, Jiaxuan You, Matei A. Zaharia, Michael Zhang, Tianyi Zhang, Xikun Zhang, Yuhui Zhang, Lucia Zheng, Kaitlyn Zhou, and Percy Liang. On the opportunities and risks of foundation models. *ArXiv*, abs/2108.07258, 2021.
- [2] Yoshua Bengio, Aaron C. Courville, and Pascal Vincent. Representation learning: A review and new perspectives. *IEEE Transactions on Pattern Analysis and Machine Intelligence*, 35:1798–1828, 2012.
- [3] Francesco Locatello, Ben Poole, Gunnar Rätsch, Bernhard Scholkopf, Olivier Bachem, and Michael Tschannen. Weakly-supervised disentanglement without compromises. In *International Conference on Machine Learning*, 2020.
- [4] Mahmut Kaya and Hasan S. Bilge. Deep metric learning: A survey. *Symmetry*, 11:1066, 2019.
- [5] Urvashi Khandelwal, Omer Levy, Dan Jurafsky, Luke Zettlemoyer, and Mike Lewis. Generalization through memorization: Nearest neighbor language models. *ArXiv*, abs/1911.00172, 2020.
- [6] Urvashi Khandelwal, Angela Fan, Dan Jurafsky, Luke Zettlemoyer, and Mike Lewis. Nearest neighbor machine translation. *ArXiv*, abs/2010.00710, 2021.
- [7] Edouard Grave, Armand Joulin, and Nicolas Usunier. Improving neural language models with a continuous cache. *ArXiv*, abs/1612.04426, 2017.
- [8] Uri Alon, Frank F. Xu, Junxian He, Sudipta Sengupta, Dan Roth, and Graham Neubig. Neuro-symbolic language modeling with automaton-augmented retrieval. In *International Conference on Machine Learning*, 2022.
- [9] Ian J. Goodfellow, Mehdi Mirza, Xia Da, Aaron C. Courville, and Yoshua Bengio. An empirical investigation of catastrophic forgetting in gradient-based neural networks. *CoRR*, abs/1312.6211, 2013.
- [10] Neil Houlsby, Andrei Giurgiu, Stanislaw Jastrzebski, Bruna Morrone, Quentin de Laroussilhe, Andrea Gesmundo, Mona Attariyan, and Sylvain Gelly. Parameter-efficient transfer learning for nlp. *ArXiv*, abs/1902.00751, 2019.

- [11] Joe Davison. Compacter: Efficient low-rank hypercomplex adapter layers. In *Neural Information Processing Systems*, 2021.
- [12] J. Edward Hu, Yelong Shen, Phillip Wallis, Zeyuan Allen-Zhu, Yuanzhi Li, Shean Wang, and Weizhu Chen. Lora: Low-rank adaptation of large language models. *ArXiv*, abs/2106.09685, 2021.
- [13] Qingru Zhang, Minshuo Chen, Alexander W. Bukharin, Nikos Karampatziakis, Pengcheng He, Yu Cheng, Weizhu Chen, and Tuo Zhao. Adalora: Adaptive budget allocation for parameter-efficient fine-tuning. 2023.
- [14] Shih yang Liu, Chien-Yi Wang, Hongxu Yin, Pavlo Molchanov, Yu-Chiang Frank Wang, Kwang-Ting Cheng, and Min-Hung Chen. Dora: Weight-decomposed low-rank adaptation. *ArXiv*, abs/2402.09353, 2024.
- [15] Haokun Liu, Derek Tam, Mohammed Muqeeth, Jay Mohta, Tenghao Huang, Mohit Bansal, and Colin Raffel. Few-shot parameter-efficient fine-tuning is better and cheaper than in-context learning. *ArXiv*, abs/2205.05638, 2022.
- [16] Yuning Mao, Lambert Mathias, Rui Hou, Amjad Almahairi, Hao Ma, Jiawei Han, Wen tau Yih, and Madian Khabsa. Unipelt: A unified framework for parameter-efficient language model tuning. In *Annual Meeting of the Association for Computational Linguistics*, 2021.
- [17] Junxian He, Chunting Zhou, Xuezhe Ma, Taylor Berg-Kirkpatrick, and Graham Neubig. Towards a unified view of parameter-efficient transfer learning. *ArXiv*, abs/2110.04366, 2021.
- [18] Irina Higgins, David Amos, David Pfau, Sébastien Racanière, Loïc Matthey, Danilo Jimenez Rezende, and Alexander Lerchner. Towards a definition of disentangled representations. *ArXiv*, abs/1812.02230, 2018.
- [19] Xingyu Cai, Jiaji Huang, Yu-Lan Bian, and Kenneth Ward Church. Isotropy in the contextual embedding space: Clusters and manifolds. In *International Conference on Learning Representations*, 2021.
- [20] Jie Hu, Li Shen, Samuel Albanie, Gang Sun, and Enhua Wu. Squeeze-and-excitation networks. *2018 IEEE/CVF Conference on Computer Vision and Pattern Recognition*, pages 7132–7141, 2017.
- [21] Alec Radford, Jeff Wu, Rewon Child, David Luan, Dario Amodei, and Ilya Sutskever. Language models are unsupervised multitask learners. 2019.
- [22] Stella Biderman, Hailey Schoelkopf, Quentin G. Anthony, Herbie Bradley, Kyle O’Brien, Eric Hallahan, Mohammad Aflah Khan, Shivanshu Purohit, USVSN Sai Prashanth, Edward Raff, Aviya Skowron, Lintang Sutawika, and Oskar van der Wal. Pythia: A suite for analyzing large language models across training and scaling. *ArXiv*, abs/2304.01373, 2023.
- [23] Xiang Zhang, Junbo Jake Zhao, and Yann LeCun. Character-level convolutional networks for text classification. In *Neural Information Processing Systems*, 2015.
- [24] Bo Pang and Lillian Lee. A sentimental education: Sentiment analysis using subjectivity summarization based on minimum cuts. *ArXiv*, cs.CL/0409058, 2004.
- [25] Ellen M. Voorhees and Dawn M. Tice. Building a question answering test collection. In *Annual International ACM SIGIR Conference on Research and Development in Information Retrieval*, 2000.
- [26] Xuan Hieu Phan, Minh Le Nguyen, and Susumu Horiguchi. Learning to classify short and sparse text & web with hidden topics from large-scale data collections. In *The Web Conference*, 2008.
- [27] Bo Pang and Lillian Lee. Seeing stars: Exploiting class relationships for sentiment categorization with respect to rating scales. In *Annual Meeting of the Association for Computational Linguistics*, 2005.
- [28] Richard Socher, Alex Perelygin, Jean Wu, Jason Chuang, Christopher D. Manning, A. Ng, and Christopher Potts. Recursive deep models for semantic compositionality over a sentiment treebank. In *Conference on Empirical Methods in Natural Language Processing*, 2013.
- [29] William B. Dolan and Chris Brockett. Automatically constructing a corpus of sentential paraphrases. In *International Joint Conference on Natural Language Processing*, 2005.

- [30] Sewon Min, Xinxi Lyu, Ari Holtzman, Mikel Artetxe, Mike Lewis, Hannaneh Hajishirzi, and Luke Zettlemoyer. Rethinking the role of demonstrations: What makes in-context learning work? *ArXiv*, abs/2202.12837, 2022.
- [31] Benfeng Xu, Quan Wang, Zhendong Mao, Yajuan Lyu, Qiaoqiao She, and Yongdong Zhang. knn prompting: Beyond-context learning with calibration-free nearest neighbor inference. *ArXiv*, abs/2303.13824, 2023.
- [32] Aston Zhang, Yi Tay, Shuai Zhang, Alvin Chan, Anh Tuan Luu, Siu Cheung Hui, and Jie Fu. Beyond fully-connected layers with quaternions: Parameterization of hypercomplex multiplications with $1/n$ parameters. *ArXiv*, abs/2102.08597, 2021.
- [33] Yao Lu, Max Bartolo, Alastair Moore, Sebastian Riedel, and Pontus Stenetorp. Fantastically ordered prompts and where to find them: Overcoming few-shot prompt order sensitivity. *ArXiv*, abs/2104.08786, 2021.
- [34] Adam Paszke, Sam Gross, Francisco Massa, Adam Lerer, James Bradbury, Gregory Chanan, Trevor Killeen, Zeming Lin, Natalia Gimelshein, Luca Antiga, Alban Desmaison, Andreas Köpf, Edward Yang, Zach DeVito, Martin Raison, Alykhan Tejani, Sasank Chilamkurthy, Benoit Steiner, Lu Fang, Junjie Bai, and Soumith Chintala. Pytorch: An imperative style, high-performance deep learning library. In *Neural Information Processing Systems*, 2019.
- [35] Thomas Wolf, Lysandre Debut, Victor Sanh, Julien Chaumond, Clement Delangue, Anthony Moi, Pierric Cistac, Tim Rault, Rémi Louf, Morgan Funtowicz, and Jamie Brew. Transformers: State-of-the-art natural language processing. In *Conference on Empirical Methods in Natural Language Processing*, 2019.
- [36] Tim Dettmers, Artidoro Pagnoni, Ari Holtzman, and Luke Zettlemoyer. Qlora: Efficient finetuning of quantized llms. *ArXiv*, abs/2305.14314, 2023.
- [37] Xiaoxia Wu, Cheng Li, Reza Yazdani Aminabadi, Zhewei Yao, and Yuxiong He. Understanding int4 quantization for language models: Latency speedup, composability, and failure cases. In *International Conference on Machine Learning*, 2023.
- [38] Georgios Arvanitidis, Lars Kai Hansen, and Søren Hauberg. Latent space oddity: on the curvature of deep generative models. *arXiv: Machine Learning*, 2017.

A Implementation Details

A.1 Stats of Language Models

The stats of language models in our experiments are shown in Table 5.

TABLE 5: Stats of GPT2 and Pythia Language Models.

	GPT2				Pythia					
	Small	Medium	Large	XL	Small	Medium	Large	XL	3B	7B
Parameters	117M	345M	762M	1.5B	160M	410M	1.0B	1.4B	2.8B	6.9B
Num. of Layer	12	24	36	48	12	24	16	24	32	32
Dimension Size	768	1,024	1,280	1,600	768	1,024	2,048	2,048	2,560	4,096
Vocabulary Size	50,257				50,304				50,432	

A.2 Stats of Datasets

The stats of datasets in our experiments are shown in Table 6.

TABLE 6: Stats of Datasets, and Number of Allowed Shots.

		AGNews	MR	MRPC	SST5	SUBJ	TREC	WebSS
Num. of Classes		4	2	2	5	2	6	8
Class Balance		✓	✓	✗	✗	✓	✗	✗
Avg. Length of Prompts		59.2	31.9	63.2	29.0	34.1	16.4	29.9
Num. of Data	Train	120,000	8,662	4,076	8,544	8,000	5,452	10,060
	Test	7,600	2,000	1,725	2,210	2,000	500	2,280
Num. of Shots	1k-context	2	8	4	4	8	8	2
	2k-context	4	16	8	8	16	16	4

A.3 Prompt Templates

The prompt templates follow the practice of prior work [33], as shown in Table 7.

TABLE 7: Prompt Template and Label Space in the Experiments.

Dataset	Prompt	Label Space
AGNews	<i>Input:</i> Nets get Carter from Raptors. "INDIANAPOLIS – All-Star Vince Carter was traded by the Toronto Raptors to the New Jersey Nets for Alonzo Mourning, Eric Williams, Aaron Williams, and a pair of first-round draft picks yesterday." <i>Type:</i> business	world, sports, business, technology
MR	<i>review:</i> "provides a porthole into that noble , trembling incoherence that defines us all ." <i>sentiment:</i> positive	negative, positive
MRPC	<i>Premise:</i> The 30-year bond US30YT = RR rose 22 / 32 for a yield of 4.31 percent , versus 4.35 percent at Wednesday 's close . <i>Hypothesis:</i> The 30-year bond US30YT = RR grew 1-3 / 32 for a yield of 4.30 percent , down from 4.35 percent late Wednesday . <i>Prediction:</i> not equivalent	equivalent, not equivalent
SST5	<i>review:</i> a deliciously nonsensical comedy about a city coming apart at its seams . <i>sentiment:</i> great	terrible, bad, okay, good, great
SUBJ	<i>input:</i> "looking for a short cut to fame , glass concocted sources , quotes and even entire stories , but his deception did not go unnoticed forever , and eventually , his world came crumbling down . . ." <i>type:</i> objective	subjective, objective
TREC	<i>Question:</i> What currency is used in Australia ? <i>Type:</i> entity	description, entity, expression, human, location, number
WebSS	<i>input:</i> americangymnasticsclub american gymnastic club recreational gymnastics boys girls schedule fees programs calendar birthday parties camps staff <i>type:</i> sports	business, computers, culture-arts-entertainment, education-science, engineering, health, politics-society, sports

A.4 Hyperparameters

In the demonstration selection, we randomly sample data from the training set. Following the practice of KP, we compute the maximum allowed number of demonstrations by setting the threshold of the

truncation probability to be 5%. We stabilize the random number by setting the random seed as the default value of 42.

In the learning process of PEFT methods, we follow the recommended practices of LORA and IA³ based on their papers. That is, making the query-key-value matrices trainable in LORA, and also making the second fully-connected layer in the feed-forward module trainable in IA³. Considering the finetuning is on the whole LM, we take the commonly used hyperparameters, letting the epoch number be 1 and the batch size be 1.

In the learning process of our approach SC, since the neural clustering module only works in the last layer, we can make its learning process separated from the LM. We take larger hyperparameters for semantic clustering: the epoch number is 100 and the batch size is 256.

A.5 Environments

Our implementation uses deep learning framework PYTORCH [34], TRANSFORMERS [35]. The experiments are conducted on Nvidia A100 GPU (80 GB).

In the experiments with Pythia-7B, we apply INT4 quantization to reduce the memory cost (while maintaining the model performance) [36, 37]. The LM quantization is dependent on the PEFT¹ library. We load LMs of other scales as they are.

B Discussion

B.1 General Semantic Basis

Considering the semantic basis is based on the LM vocabulary, we can duplicate the practice on the LM last-layer (after the last-layer, before LM-head) to the LM embedding-layer (after the embedding layer, before the first-layer) as well. For the sake of the opposite computation direction of representation, the semantic basis can be obtained by a matrix multiplication between onehot embedding and the embedding matrix. That is, we multiply the onehot embedding \vec{e} by the embedding matrix \mathbb{W} to obtain the corresponding representation \vec{r} . Expressed in formula, that is, $\vec{r} = \vec{e} \cdot \mathbb{W}$.

B.2 Entanglement and Dimension

For disentangled data, if the meaning of its dimension changes, making the elements no longer independent of each other, then it will become entangled. In LM training, when the gradient is computed, it is disentangled and each of its elements has a clear meaning (that is, the difference to the corresponding label in the vocabulary). However, passing through the LM-head, the dimension of the gradients changed, and the meaning of the dimension also changed. Therefore, the backpropagated gradient in latent space is entangled. Then, without considering the LM-head, we cannot optimize the gradients in an element-wise way, which is essential when refining the latent representations on-the-fly. As a countermeasure, we compute the gradients in the latent space, so each element of gradients has the same meaning of the dimension.

B.3 Logits and Gradients in Latent Space

The insights motivating our approach is disentanglement. In our approach of *vocabulary-defined semantics*, we compute logits and gradients *before*, instead of *after*, the LM-head. Therefore, we can disentangle the gradients in latent space, and also obtain the logits in the latent space.

In latent space, the disentangled logits are useful to analyze and evaluate latent representations, while the disentangled gradients are useful to optimize latent representations. Our approach is leveraging the vocabulary to define the semantics of LM latent space, especially the LM last-layer, therefore, we mainly guarantee the usefulness in the LM last-layer (and also embedding-layer).

¹<https://github.com/huggingface/peft>

C More Results and Analysis

C.1 The Quality of Representation Clustering

Since the clustering quality is promoted by semantic clustering. We can anticipate that, for retrieval-augmented methods, the performance will also benefit from semantic clustering.

For ease of description, we use “sibling” to describe data representations that correspond to the same label in the vocabulary, and use “neighbor” to describe data representations that are close to each other in latent space. In the process of semantic clustering, for each data, its siblings are gradually becoming its neighbors.

TABLE 8: Accuracy with k Nearest-Neighbor Methods.

Dataset	Param	GPT2				Pythia					
		Small	Medium	Large	XL	Small	Medium	Large	XL	3B	7B
AGNews	k=1 [w/o]	0.702	0.719	0.760	0.761	0.761	0.771	0.732	0.781	0.790	0.760
	k=1 [w/]	0.919	0.923	0.925	0.928	0.844	0.918	0.931	0.931	0.931	0.932
	k=16 [w/o]	0.817	0.814	0.848	0.845	0.834	0.852	0.832	0.865	0.871	0.856
	k=16 [w/]	0.922	0.927	0.926	0.930	0.885	0.921	0.932	0.934	0.934	0.935
	k=256 [w/o]	0.852	0.855	0.876	0.875	0.862	0.876	0.860	0.886	0.893	0.880
	k=256 [w/]	0.922	0.927	0.926	0.931	0.891	0.921	0.932	0.935	0.934	0.935
WebSS	k=1 [w/o]	0.255	0.293	0.424	0.396	0.416	0.423	0.404	0.449	0.428	0.370
	k=1 [w/]	0.747	0.752	0.778	0.775	0.299	0.758	0.795	0.769	0.789	0.763
	k=16 [w/o]	0.376	0.461	0.637	0.621	0.634	0.664	0.632	0.682	0.670	0.611
	k=16 [w/]	0.749	0.754	0.780	0.777	0.424	0.768	0.812	0.769	0.791	0.767
	k=256 [w/o]	0.601	0.638	0.753	0.739	0.786	0.783	0.754	0.787	0.771	0.759
	k=256 [w/]	0.789	0.795	0.818	0.812	0.528	0.807	0.852	0.806	0.828	0.807

We experimented with semantic clustering to validate its effects on nearest-neighbor methods, that is, predicting the class of data representations with the reference to the nearest neighboring data in the latent space. As shown in Table 8, there are obvious improvements in the performance when we apply semantic clustering. When the neighboring number k increased from $k = 1$ to $k = 256$, the performance of [w/o] is gradually increased and becomes closer to that of [w/]. The accuracy changes shown on [w/o] mean, that semantic clustering transforms the representations to make more neighboring data be the sibling data.

TABLE 9: LM Performance w/ and w/o Semantic Clustering.

Dataset	Metric	GPT2				Pythia					
		Small	Medium	Large	XL	Small	Medium	Large	XL	3B	7B
AGNews	ARI [w/o]	0.027	0.001	0.324	0.269	0.068	0.304	0.408	0.407	0.417	0.341
	ARI [w/]	0.806	0.816	0.812	0.826	0.711	0.806	0.831	0.834	0.833	0.835
MR	ARI [w/o]	0.188	0.171	0.379	0.270	0.000	0.082	0.382	0.074	0.365	0.039
	ARI [w/]	0.314	0.469	0.525	0.565	0.000	0.296	0.487	0.559	0.573	0.546
MRPC	ARI [w/o]	0.0	-0.006	-0.001	0.000	0.000	0.000	-0.001	0.000	0.000	0.000
	ARI [w/]	0.115	0.087	0.111	0.118	0.000	0.095	0.128	0.114	0.146	0.172
SST5	ARI [w/o]	0.000	0.000	0.000	0.002	0.000	0.039	0.083	0.069	0.150	0.037
	ARI [w/]	0.121	0.161	0.178	0.179	0.160	0.121	0.164	0.188	0.242	0.193
SUBJ	ARI [w/o]	0.021	0.257	0.012	0.000	0.000	0.057	0.047	0.192	0.173	0.002
	ARI [w/]	0.637	0.752	0.676	0.684	0.000	0.649	0.712	0.778	0.780	0.830
TREC	ARI [w/o]	0.001	0.045	0.135	0.064	0.043	0.089	0.198	0.189	0.341	0.154
	ARI [w/]	0.778	0.844	0.844	0.886	0.558	0.802	0.894	0.917	0.883	0.873
WebSS	ARI [w/o]	0.000	0.001	0.201	0.204	0.054	0.209	0.228	0.194	0.213	0.087
	ARI [w/]	0.576	0.586	0.631	0.622	0.000	0.603	0.669	0.606	0.651	0.602

We can also measure the quality of representation clustering via clustering metrics, such as *Adjusted Rand Index (ARI)*. The value range is $[-1, 1]$, the larger, the better. A value close to 0 indicates a normal disordered situation.

The results are shown in Table 9, where we use labels in the form of $llm[identifier]$ to mark variants, and identifier is either *w/o* or *w/*, representing whether semantic clustering is applied. We can see that semantic clustering can bring obvious improvements in the clustering quality.

C.2 More Results on Ablation Study

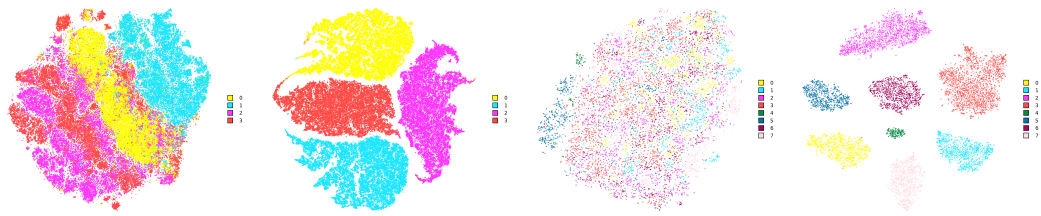
More results on the ablation study are shown in Table 10, where the conclusion consists of what we discussed in Section 5. The results show that SC has similar performance with SC[sm][mm], proving no differences between the two ways of logits computation. It is reasonable since we are merely making use of the pseudoinverse matrix to realize a transform in the computation. Then, SC[mm][sm] performs slightly worse, showing the importance of involving LM-head into consideration. Last, SC[exp-mm][sm] tends to have a bad performance, which indicates it is sensitive to the value differences with vocabulary labels. It emphasizes the usefulness of gradients disentanglement as discussed. Besides, as shown by the similar performance of SC[gt-sm][sm] and SC[exp-sm][sm], the gradients disentanglement can further reduce the costs in logits computation, since we can merely compare the results with the ground truth, instead of all labels in the vocabulary.

TABLE 10: Accuracy on Text Understanding with RAG Methods.

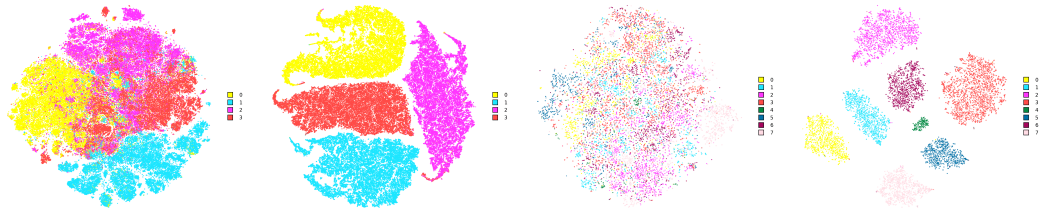
Dataset	Method	GPT2				Pythia					
		Small	Medium	Large	XL	Small	Medium	Large	XL	3B	7B
AGNews	SC	0.922	0.926	0.924	0.930	0.881	0.921	0.932	0.934	0.933	0.934
	SC[sm][mm]	0.922	0.926	0.924	0.930	0.881	0.921	0.932	0.933	0.933	0.933
	SC[mm][sm]	0.918	0.922	0.926	0.924	0.893	0.920	0.924	0.933	0.929	0.934
	SC[gt-sm][sm]	0.919	0.923	0.924	0.928	0.894	0.924	0.928	0.933	0.931	0.936
	SC[exp-mm][sm]	0.250	0.250	0.250	0.250	0.250	0.250	0.250	0.250	0.250	0.250
	SC[exp-sm][sm]	0.923	0.925	0.925	0.928	0.879	0.922	0.927	0.929	0.937	0.936
MR	SC	0.781	0.843	0.863	0.876	0.500	0.772	0.849	0.874	0.879	0.870
	SC[sm][mm]	0.781	0.843	0.863	0.876	0.500	0.772	0.849	0.874	0.879	0.870
	SC[mm][sm]	0.770	0.771	0.829	0.856	0.500	0.788	0.841	0.867	0.819	0.824
	SC[gt-sm][sm]	0.770	0.826	0.831	0.873	0.500	0.791	0.818	0.872	0.874	0.860
	SC[exp-mm][sm]	0.500	0.500	0.500	0.500	0.500	0.500	0.500	0.500	0.500	0.500
	SC[exp-sm][sm]	0.772	0.832	0.861	0.876	0.500	0.770	0.853	0.874	0.879	0.867
MRPC	SC	0.681	0.659	0.674	0.681	0.665	0.678	0.697	0.682	0.703	0.717
	SC[sm][mm]	0.681	0.658	0.674	0.681	0.665	0.678	0.697	0.682	0.703	0.717
	SC[mm][sm]	0.632	0.688	0.686	0.712	0.517	0.675	0.693	0.692	0.704	0.726
	SC[gt-sm][sm]	0.690	0.698	0.706	0.705	0.687	0.666	0.699	0.708	0.631	0.733
	SC[exp-mm][sm]	0.665	0.335	0.665	0.335	0.665	0.685	0.665	0.665	0.665	0.665
	SC[exp-sm][sm]	0.689	0.667	0.702	0.691	0.665	0.677	0.703	0.705	0.711	0.719
SSTS	SC	0.418	0.456	0.479	0.480	0.452	0.419	0.463	0.478	0.480	0.495
	SC[sm][mm]	0.418	0.456	0.479	0.478	0.453	0.419	0.462	0.480	0.482	0.492
	SC[mm][sm]	0.420	0.460	0.475	0.462	0.435	0.406	0.439	0.475	0.462	0.457
	SC[gt-sm][sm]	0.421	0.482	0.470	0.466	0.446	0.415	0.483	0.471	0.480	0.468
	SC[exp-mm][sm]	0.286	0.286	0.286	0.286	0.231	0.176	0.231	0.231	0.286	0.231
	SC[exp-sm][sm]	0.413	0.450	0.467	0.461	0.429	0.432	0.452	0.491	0.476	0.472
SUBJ	SC	0.899	0.934	0.911	0.914	0.500	0.903	0.922	0.941	0.942	0.956
	SC[sm][mm]	0.899	0.934	0.911	0.914	0.500	0.903	0.922	0.941	0.942	0.956
	SC[mm][sm]	0.885	0.889	0.899	0.914	0.500	0.922	0.926	0.943	0.833	0.500
	SC[gt-sm][sm]	0.912	0.941	0.932	0.944	0.500	0.854	0.931	0.935	0.945	0.941
	SC[exp-mm][sm]	0.500	0.500	0.500	0.500	0.500	0.500	0.500	0.500	0.500	0.500
	SC[exp-sm][sm]	0.892	0.934	0.928	0.939	0.500	0.895	0.935	0.937	0.932	0.957
TREC	SC	0.908	0.934	0.932	0.952	0.784	0.916	0.956	0.964	0.950	0.946
	SC[sm][mm]	0.908	0.932	0.932	0.952	0.784	0.916	0.956	0.964	0.948	0.948
	SC[mm][sm]	0.910	0.920	0.936	0.944	0.848	0.918	0.954	0.956	0.958	0.948
	SC[gt-sm][sm]	0.894	0.948	0.924	0.954	0.796	0.894	0.954	0.952	0.958	0.952
	SC[exp-mm][sm]	0.130	0.188	0.130	0.276	0.276	0.348	0.130	0.654	0.498	0.226
	SC[exp-sm][sm]	0.900	0.934	0.930	0.956	0.784	0.924	0.960	0.956	0.948	0.952
WebSS	SC	0.792	0.796	0.818	0.811	0.132	0.807	0.845	0.807	0.829	0.807
	SC[sm][mm]	0.791	0.794	0.814	0.811	0.132	0.804	0.843	0.807	0.830	0.804
	SC[mm][sm]	0.797	0.780	0.781	0.779	0.132	0.793	0.791	0.811	0.811	0.801
	SC[gt-sm][sm]	0.797	0.797	0.820	0.813	0.132	0.805	0.849	0.828	0.825	0.812
	SC[exp-mm][sm]	0.132	0.132	0.132	0.132	0.132	0.132	0.132	0.132	0.132	0.132
	SC[exp-sm][sm]	0.785	0.794	0.818	0.806	0.132	0.809	0.803	0.824	0.816	0.806
Avg.	SC	0.771	0.792	0.800	0.806	0.559	0.774	0.809	0.811	0.816	0.818
	SC[sm][mm]	0.771	0.792	0.800	0.806	0.559	0.773	0.809	0.812	0.817	0.817
	SC[mm][sm]	0.762	0.776	0.790	0.799	0.546	0.775	0.795	0.811	0.788	0.741
	SC[gt-sm][sm]	0.772	0.802	0.801	0.812	0.565	0.764	0.809	0.814	0.806	0.815
	SC[exp-mm][sm]	0.352	0.313	0.352	0.326	0.365	0.370	0.344	0.419	0.404	0.358
	SC[exp-sm][sm]	0.767	0.791	0.804	0.808	0.555	0.775	0.805	0.816	0.814	0.815

D Representations in the Latent Space

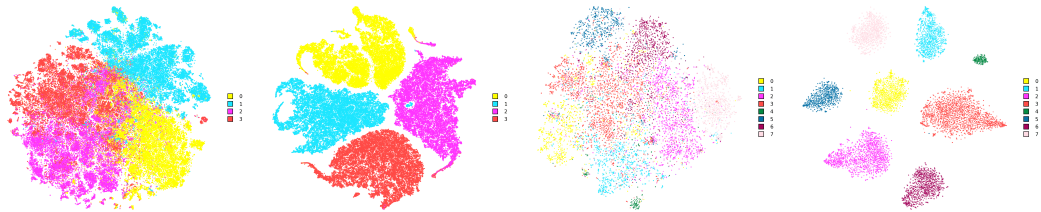
To illustrate the effects of semantic clustering, we visualize representations in the latent space using tSNE [38], mainly on the AGNews and WebSS datasets. For example, as shown in Figure 11, before semantic clustering, the data representations were messily scattered. In contrast, after semantic clustering, the representations scatter into a few clusters, and in each cluster, the representations correspond to the same semantic meaning. However, in some models, such as Figure 6, the clustering effects are not that good. It explains why semantic clustering performs badly with the Pythia-S model.



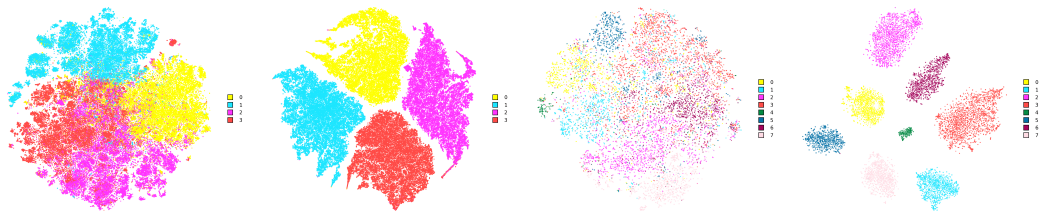
(a) on AGNews w/o SC (b) on AGNews w/ SC (c) on WebSS w/o SC (d) on WebSS w/ SC
 Figure 2: tSNE Illustration of Semantic Clustering in GPT2-S Latent Space.



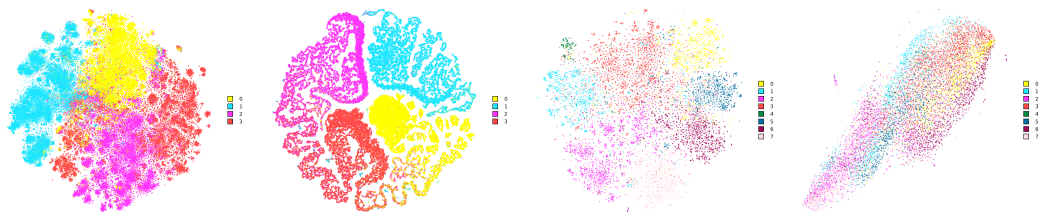
(a) on AGNews w/o SC (b) on AGNews w/ SC (c) on WebSS w/o SC (d) on WebSS w/ SC
 Figure 3: tSNE Illustration of Semantic Clustering in GPT2-M Latent Space.



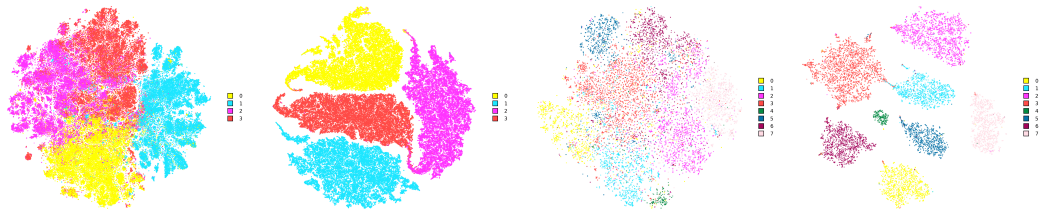
(a) on AGNews w/o SC (b) on AGNews w/ SC (c) on WebSS w/o SC (d) on WebSS w/ SC
 Figure 4: tSNE Illustration of Semantic Clustering in GPT2-L Latent Space.



(a) on AGNews w/o SC (b) on AGNews w/ SC (c) on WebSS w/o SC (d) on WebSS w/ SC
 Figure 5: tSNE Illustration of Semantic Clustering in GPT2-XL Latent Space.

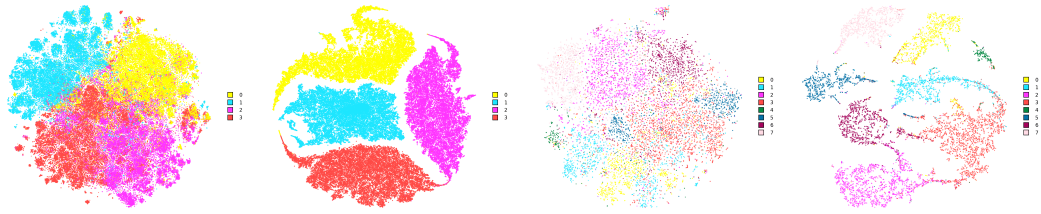


(a) on AGNews w/o SC (b) on AGNews w/ SC (c) on WebSS w/o SC (d) on WebSS w/ SC
 Figure 6: tSNE Illustration of Semantic Clustering in Pythia-S Latent Space.



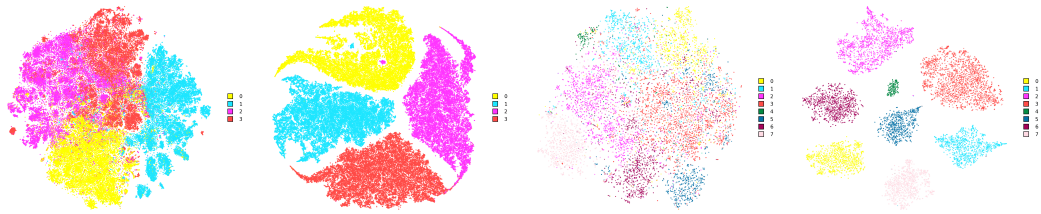
(a) on AGNews w/o SC (b) on AGNews w/ SC (c) on WebSS w/o SC (d) on WebSS w/ SC

Figure 7: tSNE Illustration of Semantic Clustering in Pythia-M Latent Space.



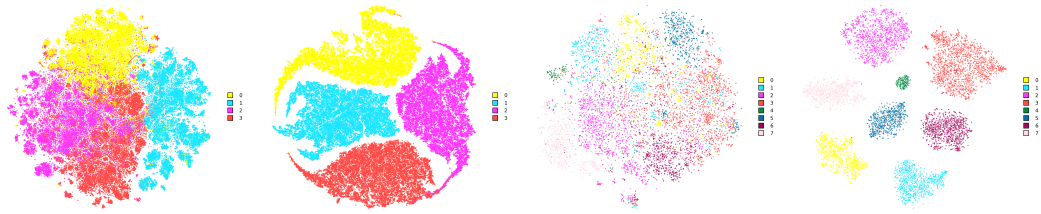
(a) on AGNews w/o SC (b) on AGNews w/ SC (c) on WebSS w/o SC (d) on WebSS w/ SC

Figure 8: tSNE Illustration of Semantic Clustering in Pythia-L Latent Space.



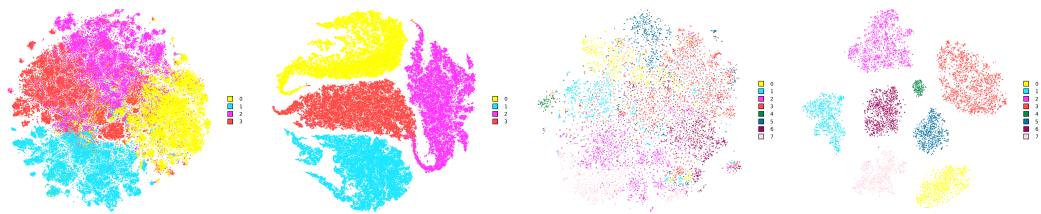
(a) on AGNews w/o SC (b) on AGNews w/ SC (c) on WebSS w/o SC (d) on WebSS w/ SC

Figure 9: tSNE Illustration of Semantic Clustering in Pythia-XL Latent Space.



(a) on AGNews w/o SC (b) on AGNews w/ SC (c) on WebSS w/o SC (d) on WebSS w/ SC

Figure 10: tSNE Illustration of Semantic Clustering in Pythia-3B Latent Space.



(a) on AGNews w/o SC (b) on AGNews w/ SC (c) on WebSS w/o SC (d) on WebSS w/ SC

Figure 11: tSNE Illustration of Semantic Clustering in Pythia-7B Latent Space.